Journal of Science and Technology in Civil Engineering, NUCE 2021. 15 (2): 127–140

NUMERICAL ANALYSIS OF SEISMIC BEHAVIOR OF SQUARE CONCRETE FILLED STEEL TUBULAR COLUMNS

Hao Dinh Phan[a,*]

[a] *Faculty of Civil Engineering, The University of Danang – University of Science and Technology, 54 Nguyen Luong Bang street, Lien Chieu district, Da Nang city, Vietnam*

Article history:
Received 24/03/2021, Revised 19/04/2021, Accepted 22/04/2021

Abstract

This paper presents a numerical analysis of the seismic behavior of square concrete filled steel tubular (CFST) columns. Finite element analysis (FEA) models in ABAQUS software were used to simulate a series of columns subjected to axial compression and cyclic lateral loading. The CFST columns were simulated using nonlinear tri-dimensional (3-D) finite elements for the infilled concrete, and nonlinear two-dimensional (2-D) finite elements for the steel tube. The feasibility of the FEA model has been validated by published experimental results. The validated FEA model was further extended to conduct parametric studies with various parameters including axial load level (n), width-to-thickness ratio of steel tube (B/t), and concrete strength. The numerical analysis results reveal that with the same B/t and constitute materials, the higher the axial compression, the lower the shear strength and deformation capacity were. The thicker steel wall ($B/t = 21$) resulted in higher strength and larger deformation capacity of the column. Increasing concrete strength helped to significantly develop the column's shear strength in all cases. Meanwhile, it just led to an increase in deformation capacity in some cases depending on n and B/t. This study also reveals that the square CFST columns with B/t of 21 satisfy the seismic performance demand in high seismic zones (ultimate interstory drift ratio (IDR_u) not less than 3% radian) under the two axial load levels, 0.35 and 0.45, but the columns with B/t of 28 satisfy the above demand under just one axial load level of 0.35.

Keywords: square concrete filled steel tubular (CFST) columns; finite element analysis (FEA) model; width-to-thickness ratio (B/t); high axial load level; seismic behavior.

https://doi.org/10.31814/stce.nuce2021-15(2)-11

1. Introduction

To have good understanding of the seismic design of concrete filled steel tubular (CFST) columns, many past studies were conducted both experimentally and analytically. In which, experimental studies have brought significant benefits with a valuable test database on the mechanical behavior and load-bearing capacity of various structural members and systems. However, there were disadvantages of experimental studies including the relevant requirements of testing facilities, specimens' fabrication time, and cost, especially for testing the full-scale specimens [1]. Hence, analytical studies have become a significant part to overcome the mentioned limitations of the experimental method. This

*Corresponding author. *E-mail address:* pdhao@dut.udn.vn (Phan, H. D.)

results in not only reducing research duration and cost but also increasing the range of comprehensive parametric studies to get a bigger database for further design applications in structural engineering.

For analytical studies, finite element analysis (FEA) modeling has been widely used with the support of some software packages. The mechanical behavior of CFST columns under different loading conditions was analytically investigated by many researchers. For axial loading, previous studies revealed that the cross-section shape and the width-(diameter)-to-thickness ratio (B/t or D/t) of steel tube significantly affected the column's loading capacity [2–5]. In which, the columns with circular sections demonstrated a better confinement effect than that with non-circular sections. Moreover, the concrete confinement effect has dramatically increased when applying axial compression on the concrete core only compared to other loading types [6–9]. To model the behavior of steel tube and infilled concrete, there were different models used in previous studies [10, 11]. For combined axial and flexural loading, the numerical analysis process was more complicated, especially in the case of cyclic loading. The mechanical behavior of CFST columns under combined axial and monotonic lateral loading was analytically studied by some researchers [12–15]. The numerical analysis conducted by Han et al. [12] showed that the axial load level affects the shear loading capacity of the steel tube. Namely, with the axial load ratio less than or equal to 0.2, the shear loading capacity of steel tube tends to increase when increasing the lateral displacement. Meanwhile, with the axial load ratio greater than or equal to 0.4, the shear loading capacity of steel tube reduces after reaching the peak load due to softening behavior. A nonlinear fiber element analysis method was developed by Liang [13] for predicting the $P - M$ interaction diagrams of CFST columns subjected to axial load and biaxial bending. Moreover, an analytical investigation on circular CFST columns under combined axial and flexural loading, which was conducted by Moon et al. [15], indicated that the predictions of CFST column's strength using current design codes are good just in the case of axial or bending demand, but conservative in the case of combined loading. The seismic behavior of CFST columns under combined axial and cyclic lateral loading was also analytically studied in recent decades [16–21]. In which, accurate modeling the behavior of steel tube and infilled concrete components was a critical challenge so far. Especially, the concrete stress-strain curve for modeling infilled concrete in CFST columns is significantly changed depending on some factors such as cross-section shape, B/t (D/t) value, material strength, and loading condition. Research by Hajjar and Gourley [16] revealed that the uniaxial stress-strain curve for infilled concrete in rectangular or square CFST columns subjected combined loading has a different shape in compressive behavior. It was shown that the lower the B/t value, the better the stress-strain curve with longer strain in the peak stress and higher stress in the post-peak portion. Zubydan and ElSabbagh [19] analytically investigated the local buckling effect of steel tube in rectangular CFST columns under combined loading. Their study results showed that neglecting the local buckling effect in modeling leads to overestimating the maximum and/or the post-peak capacity of the composite column according to the tube geometry and the constituent material properties. Another research conducted by Patel et al. [20] has developed cyclic stress-strain curves for steel tube and infilled concrete in rectangular CFST columns.

From past studies, some valuable models for both steel and concrete materials can be used to model the behavior of CFST columns under combined axial and flexural loading. However, to have an accurate confined concrete model used for infilled concrete is very difficult, especially, in the case of high and varying axial loads. Also, in Vietnam, there is a lack of reasonable concrete models proposed for simulation purpose. There were some experimental studies on this field, for example, an experimental investigation on the effectiveness of stirrup detailing on the structural performance of reinforced concrete columns was studied by [22]. In particular, to overcome the limitation of experimental database in the case of testing full-scale specimens, this study focuses on performing numerical investigations on the seismic behavior of square CFST columns with high axial load levels. The main purpose of this study is to analyze the effects of some parameters such as axial load level, width-to-thickness ratio of the steel tube, and concrete strength on the column's strength and deformation capacity.

2. Numerical modeling

2.1. Modeling procedure

To build a full CFST column model, four main steps including steel tube modeling, infilled concrete modeling, steel-concrete interaction modeling, boundary conditions with loading application need to be performed carefully to ensure that all the model components are properly connected. In which, ABAQUS [23] would be used to model the column members by using nonlinear tri-dimensional (3-D) finite elements, C3D8R, for modeling the infilled concrete component, and nonlinear two-dimensional (2-D) finite elements, S4R, for modeling the steel tube component. The element types and meshing of steel tube and infilled concrete were chosen as shown in Fig. 1. To have good analysis results, the mesh size convergence was tested to select reasonable meshes for steel and infilled concrete components. For the steel tube, the finner mesh was chosen in the areas near the Top and Bottom column ends with B distance from the footing surface as shown in Fig. 1(a). This results higher accuracy in mechanical behavior of these large deformation areas due to the local buckling of the steel walls.

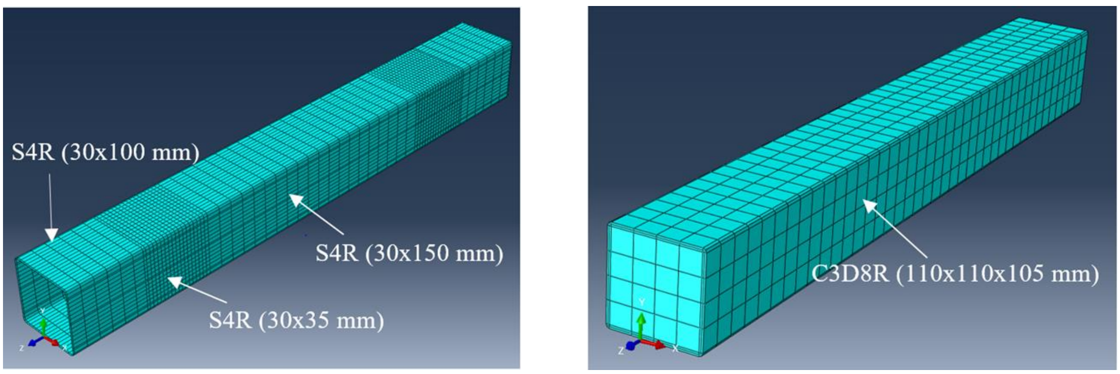

(a) The meshing of steel tube

(b) The meshing of concrete core

Figure 1. Steel tube and concrete meshing

For modeling material properties of steel tube in ABAQUS, the elastic and linear hardening plastic model as shown in Fig. 2, is reasonable to use. In the elastic stage, linear stress-strain behavior was defined based on the steel yield strength (f_y) and modulus of elasticity (E_s). In which, f_y is chosen as the nominal steel strength, and $E_s$is taken as 200 GPa with Poisson's ratio (v_s) of 0.3 in modeling.

To have rational and accurate concrete model for infilled concrete in the square CFST columns, especially with full-scale ones, is a big challenge for the simulation process. Hence, a concrete damaged plasticity (CDP) material model available in ABAQUS needs to be developed with consideration of the confinement effect for use in the modeling in this study. Because the previously confined concrete models [11, 20] could not accurately simulate the seismic behavior of full-scale square CFST columns [1], a new confined concrete model has been developed by the author. The compressive behavior of infilled concrete depends on the axial load ratio, $n = P/P_0$, in which increasing n value leads to a reduction of both the confined strength of infilled concrete (f'_{cc}) and the later confined strain at the peak stress (ε_{cc2}). The proposed confined concrete model according to $n = 0.35$ for the case of f'_c = 36.35 MPa is presented in Fig. 3.

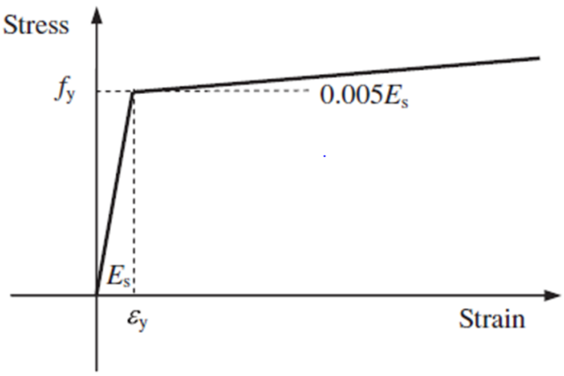

Figure 2. Stress-strain model for steel tube

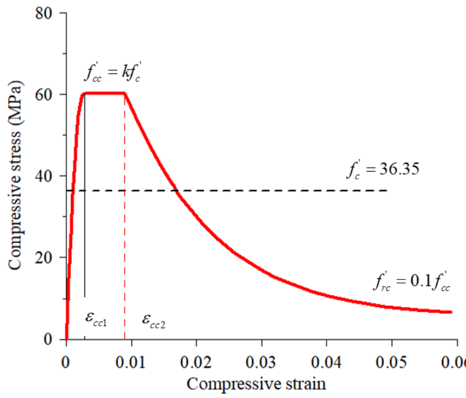

Figure 3. A proposed confined concrete model

The *Contact pair option with surface-to-surface contact type was used to model the interaction between the steel tube and infilled concrete. A pair of surfaces in this contact including master and slave surfaces requires to be defined. To reduce numerical errors, the slave surface should belong to a softer component, the steel tube, and has a finer mesh than the master one, the infilled concrete [23]. The contact property between the master and slave surfaces was defined by normal behavior and tangential behavior. In which, the normal behavior is simulated by the "Hard" contact which allows for the separation of the two surfaces after contact. The tangential behavior between the two surfaces is simulated by the Coulomb friction model with a friction coefficient taken as 0.25 [24]. Steel-concrete interaction modeling is shown in Fig. 4.

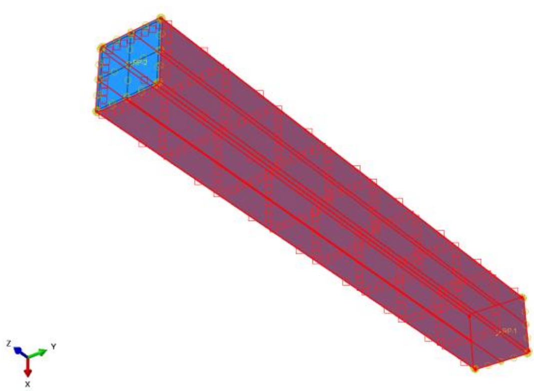

(a) Outside surfaces of infilled concrete (master surfaces)

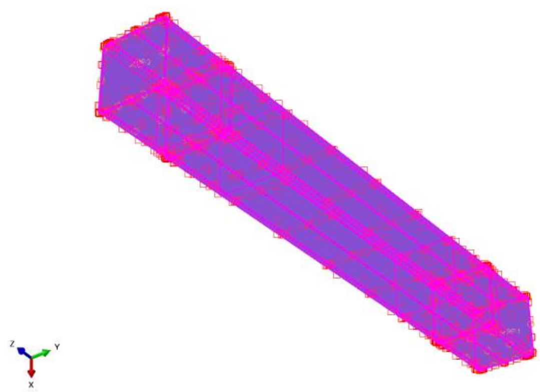

(b) Inside surfaces of steel tube (slave surfaces)

Figure 4. Steel-concrete interaction modeling

The square CFST column specimens tested in Phan and Lin [1] were fully fixed at the Top end and partially fixed at the Bottom end with releases of one degree of freedom (DOF) with moving along the axial axis (longitudinal direction) of the column and another DOF in the direction for applying cyclic lateral displacement load. In the experimental program, the fully-fixed column end was achieved using the column end connected to the top footing and then completely fixed to the cross beam of the Multi-Axial Testing System (MATS). Meanwhile, the partially-fixed column end was achieved through the column end connected to the bottom footing and then completed fixed to the platen (shaking table) of the MATS, which can be applied by the axial compression and cyclic lateral displacement loading. In modeling, the boundary conditions were applied in the two ends of the column specimen as shown in Fig. 5.

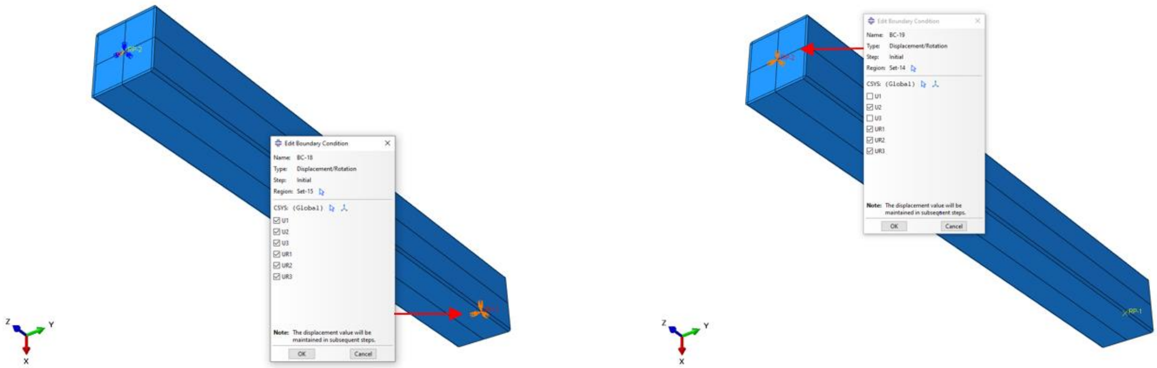

(a) Top column end with full fixing (b) Bottom column end with partial fixing

Figure 5. Boundary conditions at Top and Bottom column ends

2.2. *Parametric studies*

Table 1. Matrix of CFST column specimens

Specimen	t (mm)	B/t	$f_c^{'}$ (MPa)	$n = P/P_0{}^{(*)}$
CFST28-380/35-35C	18	28	35	0.35
CFST28-380/35-45C	18	28	35	0.45
CFST28-380/35-55C	18	28	35	0.55
CFST28-380/70-35C	18	28	70	0.35
CFST28-380/70-45C	18	28	70	0.45
CFST28-380/70-55C	18	28	70	0.55
CFST21-380/35-35C	24	21	35	0.35
CFST21-380/35-45C	24	21	35	0.45
CFST21-380/35-55C	24	21	35	0.55
CFST21-380/70-35C	24	21	70	0.35
CFST21-380/70-45C	24	21	70	0.45
CFST21-380/70-55C	24	21	70	0.55

$^{(*)}$Note: P is the axial load applied; $P_0 = A_s f_y + 0.85 A_c f_c^{'}$, the axial compressive strength of the CFST column, was defined according to AISC 360-16 [25], in which A_s and A_c is cross-section area of the steel tube and concrete core, respectively; f_y and $f_c^{'}$ is the yield stress and compressive strength of the steel tube and concrete core, respectively.

The FEA model developed using new confined concrete models proposed in this study were validated by the experimental data collected in [1] with a good agreement. To investigate the seismic behavior of square CFST columns under high axial compression, three axial load levels (n = 0.35, 0.45, and 0.55) were chosen. Two other parameters B/t and f_c' would be chosen at two levels for each parameter. For all specimens, the column length was 3000 mm, in which the outer width and yield strength of steel tubes were 500 mm and 380 MPa, respectively. The details of all parameters investigated in this study are shown in Table 1. The validated FEA model was extended to conduct parametric studies to investigate the effects of the parameters including n, B/t and f_c' as mentioned above on the strength and deformation capacity of CFST columns. The numerical results and discussions would be presented in detail in the next section.

3. Numerical results and discussions

3.1. Numerical results

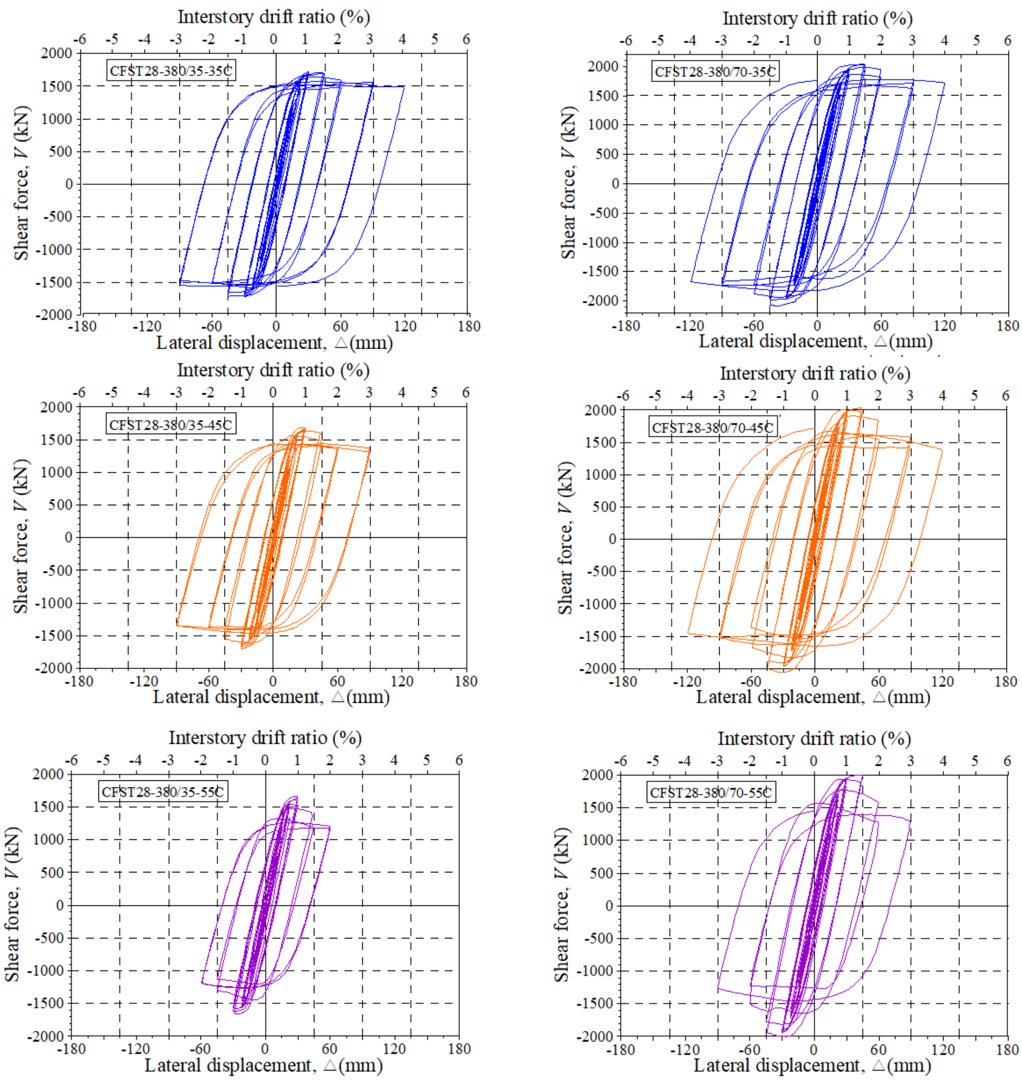

(a) CFST columns using f_c' = 35 MPa

(b) CFST columns using f_c' = 70 MPa

Figure 6. Hysteresis loops of specimens with B/t = 28

The numerical results including shear force versus lateral displacement hysteresis loops, shear strength, ultimate interstory drift ratio (IDR_u) of all specimens, and several typical failure modes of some specimens are presented below. In which, the hysteresis loops for shear force versus lateral displacement were drawn for all twelve specimens, as shown in Figs. 6 and 7. The failure modes of three specimens with B/t of 21 were shown in Fig. 8. The maximum and minimum values of shear force ($V_{\max,\min}$), and the values of IDR_u in positive and negative directions of all specimens were also calculated and presented as in Table 2.

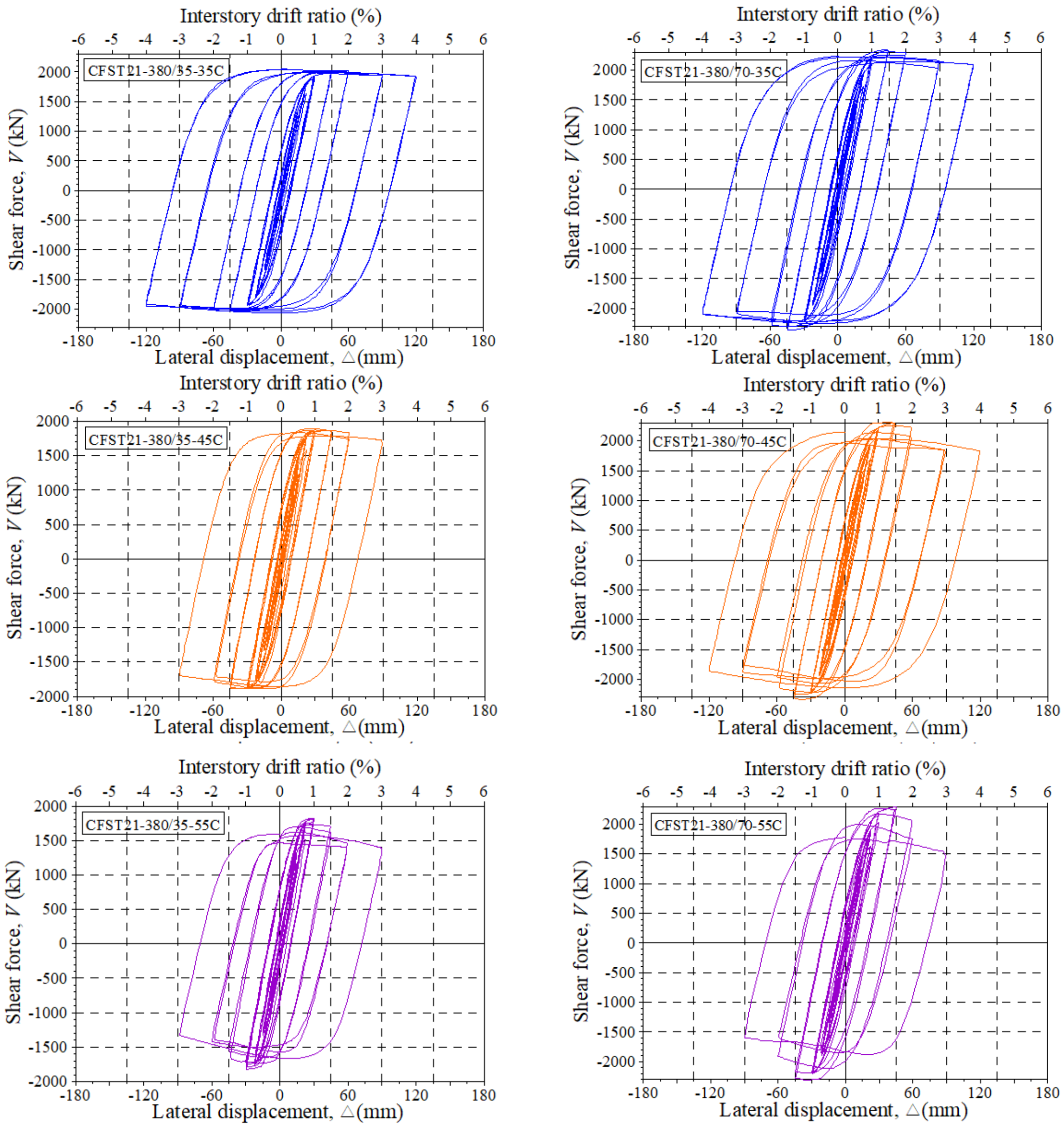

(a) CFST columns using f'_c = 35 MPa (b) CFST columns using f'_c = 70 MPa

Figure 7. Hysteresis loops of specimens with $B/t = 21$

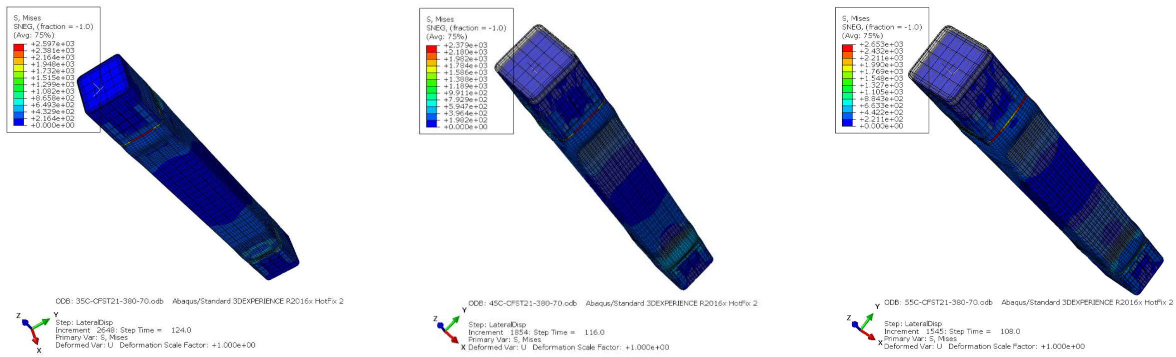

(a) Specimen CFST21-380/70-35C (b) Specimen CFST21-380/70-45C (c) Specimen CFST21-380/70-55C

Figure 8. Failure modes of three specimens with $B/t = 21$

Table 2. Numerical simulation results

Specimen	$V_{\max,\min}$ (kN)			$\mathrm{IDR_u}^{(*)}$ (%)		
	max	min	average	pos.	neg.	average
CFST28-380/35-35C	1720	−1727	1724	4.00+	3.00+	3.50+
CFST28-380/35-45C	1689	−1702	1696	3.00+	2.50	2.75+
CFST28-380/35-55C	1663	−1663	1663	1.67	1.45	1.56
CFST28-380/70-35C	2044	−2083	2064	4.00+	4.00	4.00+
CFST28-380/70-45C	2031	−2057	2044	2.83	2.50	2.67
CFST28-380/70-55C	2004	−2001	2003	1.98	1.92	1.95
CFST21-380/35-35C	2034	−2061	2048	4.00+	4.00+	4.00+
CFST21-380/35-45C	1888	−1889	1889	3.00+	3.00+	3.00+
CFST21-380/35-55C	1825	−1828	1827	2.00	2.00	2.00
CFST21-380/70-35C	2336	−2366	2351	4.00+	4.00+	4.00+
CFST21-380/70-45C	2308	−2340	2324	2.94	4.00	3.47
CFST21-380/70-55C	2293	−2277	2285	2.39	2.29	2.34

$^{(*)}$Note: $\mathrm{IDR_u}$ was defined at the point on the hysteresis loop following the post-peak trend in positive (pos.) and negative (neg.) directions, respectively, that the shear force equals 80% maximum shear force.

3.2. *Effect of axial load level*

The axial load level affects the seismic behavior of these square CFST columns such as shear strength and deformation capacity. For shear strength, as can be seen in Fig. 9, with the same B/t and f_c', the higher the axial compression, the smaller the column shear strength was. When increasing the axial load ratio from 0.35 to 0.55, the shear strength decreases more significantly with 11% in the case of lower B/t (21) and lower f_c' (35 MPa). However, the shear strength drops just between 3 and 3.5% in the remaining cases. It reveals that using a thicker steel tube with high strength steel (380 MPa) and low concrete strength (35 MPa) results in a significant reduction of shear strength under high axial load level.

For deformation capacity, the axial load level has also dramatically affected columns' deformation as shown in Fig. 10. In general, the higher the axial compression, the smaller the deformation capacity

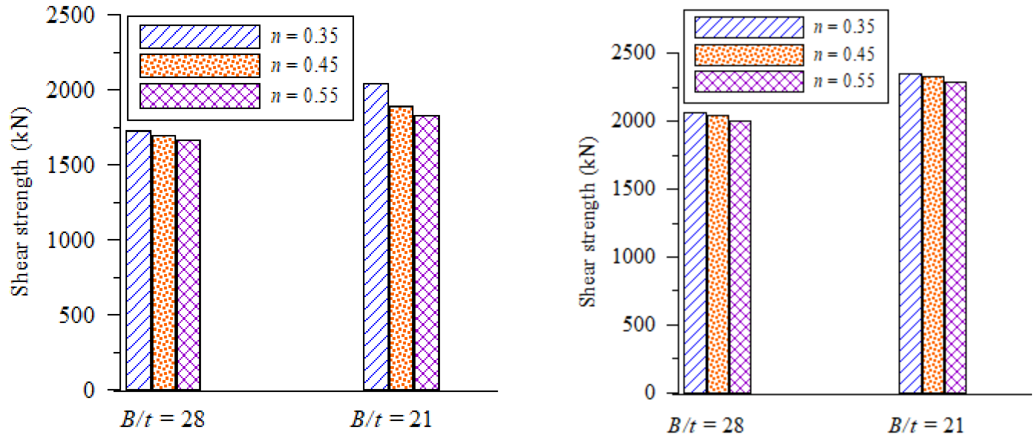

(a) Specimens with $f_c^{\prime}$ = 35 MPa (b) Specimens with $f_c^{\prime}$ = 70 MPa

Figure 9. Effect of axial load level on columns' shear strength

was. Firstly, at the lowest axial load level, n = 0.35, the ultimate interstory drift ratio (IDR_u) of all specimens was more than 3% radian, especially, it was more than 4% radian in the cases of thicker steel tubes (B/t = 21) and higher strength concrete ($f_c^{\prime}$ = 70 MPa) filled in a thinner steel tube (B/t = 28). Secondly, at the middle axial load level, n = 0.45, the columns with thicker steel tube still supports to increase IDR_u (larger than 3% radian). However, for the thinner steel tube (B/t = 28), using higher strength concrete leads to a reduction of column deformation capacity with IDR_u of 2.75+ and 2.67% radian when using infilled concrete with $f_c^{\prime}$ of 35 and 70 MPa, respectively. Thirdly, at the highest axial load level, n = 0.55, using thicker steel tubes (B/t = 21) and higher strength concrete (70 MPa) results in an increase of IDR_u value compared to other cases. However, IDR_u values could not exceed 3% radian, just from 1.56 to 2.34%.

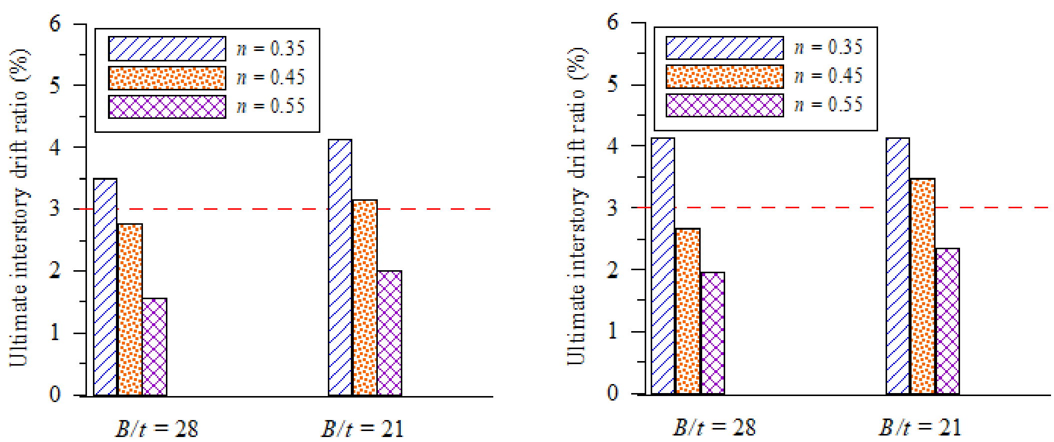

(a) Specimens with $f_c^{\prime}$ = 35 MPa (b) Specimens with $f_c^{\prime}$ = 70 MPa

Figure 10. Effect of axial load level on columns' deformation

3.3. Effect of width-to-thickness ratio

The width-to-thickness ratio of the steel tube, B/t, strongly affects the seismic performance of square CFST columns including strength and deformation capacity. A general B/t effect trend shows that the smaller the B/t of steel tube, the higher the shear strength and the deformation capacity of the CFST column were.

As shown in Fig. 11, reducing B/t value leads to an increase of shear strength for all cases of concrete strength and axial load level. For $f_c' = 35$ MPa (Fig. 11(a)), reducing B/t value from 28 down to 21 increases shear strength about 18.8, 11.4, and 9.9% for the axial load ratio of 0.35, 0.45, and 0.55, respectively. It reveals that a higher increase rate happened in the case of a lower axial load level. For $f_c' = 70$ MPa (Fig. 11(b)), the corresponding shear strength increase is 13.9, 13.7, and 14.1% at the three axial load levels ($n = 0.35$, 0.45, and 0.55), respectively. Moreover, the thicker steel tube (B/t of 21) keeps the shear strength more stable when increasing the axial load level from 0.35 to 0.55, in the case of using higher strength concrete (f_c' of 70 MPa).

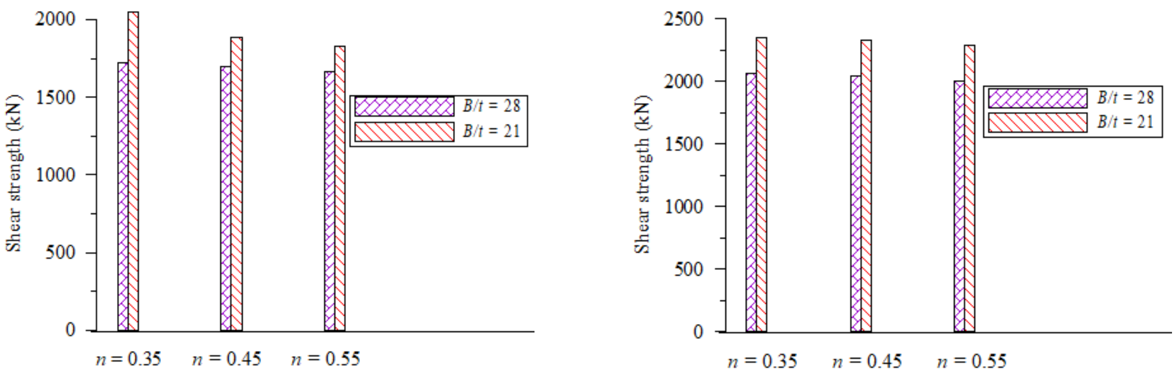

(a) Specimens with $f_c' = 35$ MPa (b) Specimens with $f_c' = 70$ MPa

Figure 11. Effect of width-to-thickness ratio on columns' shear strength

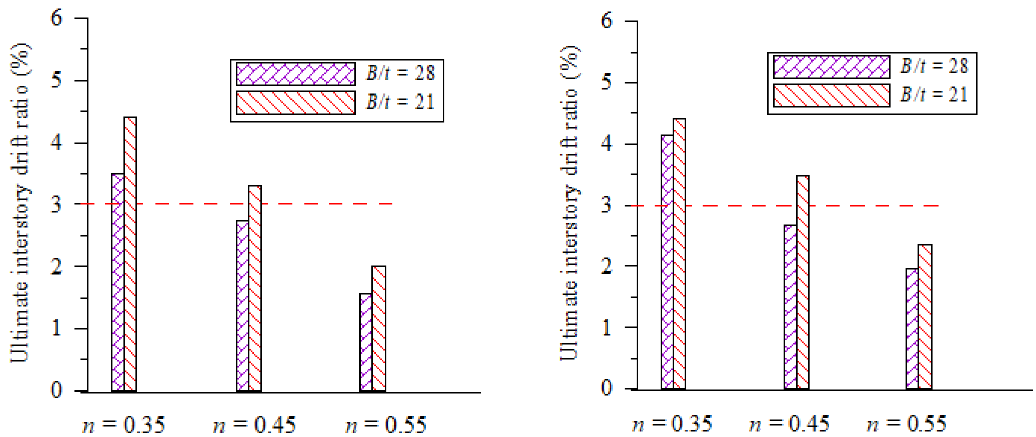

(a) Specimens with $f_c' = 35$ MPa (b) Specimens with $f_c' = 70$ MPa

Figure 12. Effect of width-to-thickness ratio on columns' deformation

The deformation comparisons in Fig. 12 were conducted between specimens in two levels of B/t, 28 and 21, using the steel tubes with fy of 380 MPa and filled with normal and high strength concrete, f_c' of 35 and 70 MPa. The comparison results show that there is an increase in the deformation capacity when reducing B/t value. In the case of f_c' = 35 MPa, reducing B/t value from 28 down to 21, the IDR_u has an increase of about 1.26, 1.15, and 1.28 times for the axial load ratio of 0.35, 0.45, and 0.55, respectively (Fig. 12(a)). In the case of f_c' = 70 MPa, reducing the B/t value from 28 down to 21, the IDR_u has an increase of about 1.06, 1.30, and 1.20 times for the axial load ratio of 0.35, 0.45, and 0.55, respectively (Fig. 12(b)).

3.4. Effect of concrete strength

The concrete strength of infilled concrete plays a significant role in the contribution to the seismic performance enhancement of the square CFST columns. The effect of concrete strength on the shear strength and deformation capacity of these composite columns is analyzed in detail as below.

Fig. 13 presents shear strength comparisons of all specimens for evaluating the effect of concrete strength. The comparison results show that increasing the concrete strength from 35 to 70 MPa leads to an enhancement of column shear strength. In which, the larger increase ratio happens in the case of CFST columns subjected to higher axial compression. Namely, for columns using thinner steel tubes (B/t = 28), the shear strength increase is 18.8, 20.2, and 20.5% in the case of n = 0.35, 0.45, and 0.55, respectively (see Fig. 13(a)). Meanwhile, for columns using thicker steel tubes (B/t = 21), it is 14.8, 22.2, and 25.6% in the case of n = 0.35, 0.45, and 0.55, respectively (see Fig. 13(b)). Hence, the largest shear strength increase occurs in the column with B/t of 21 under an axial load ratio of 0.55.

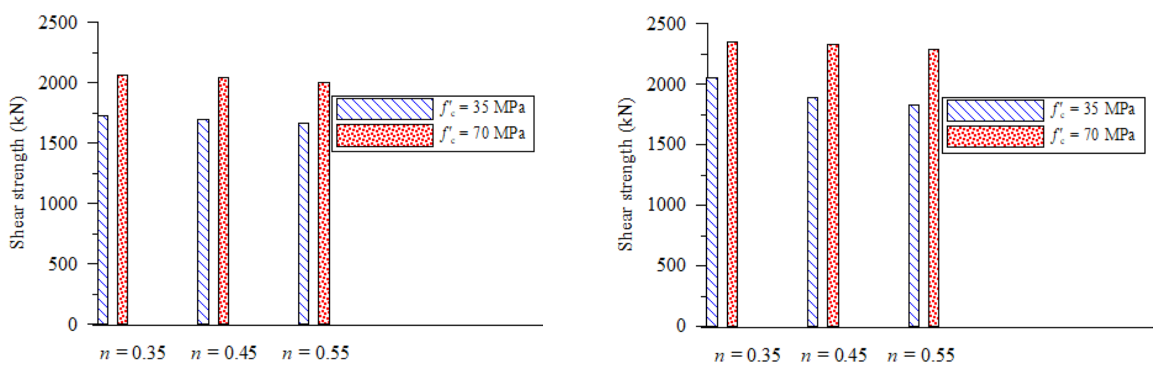

(a) Specimens with B/t = 28 (b) Specimens with B/t = 21

Figure 13. Effect of concrete strength on columns' shear strength

Fig. 14 shows deformation comparisons of all specimens for evaluating the effect of concrete strength. The comparison results show that increasing the concrete strength from 35 to 70 MPa leads to some changes in the column's deformation capacity depending on axial load level and B/t value. The deformation increase happens in the cases of B/t = 28, n = 0.35 and 0.55 and B/t = 21, n = 0.45 and 0.55, in which, the larger increase happens in the case of thinner steel tube used (Fig. 14(a)). Meanwhile, the deformation decrease happens in the cases of B/t = 28, n = 0.45 and there is no changed in the case of B/t = 21, n = 0.35 (Fig. 14(b)). Based on the comparisons, it also reveals that under higher axial compression (n = 0.45 and 0.55) the concrete strength increase could not significantly enhance the deformation capacity of the column. As shown in Fig. 14, just specimens with thicker steel tubes ($B/t = 21$) have good deformation capacity (with IDR_u higher or equal to 3% radian) at two axial load levels of 0.35 and 0.45, meanwhile, specimens with thinner steel tubes ($B/t = 28$) have IDR_u higher 3% radian at lowest axial load level only.

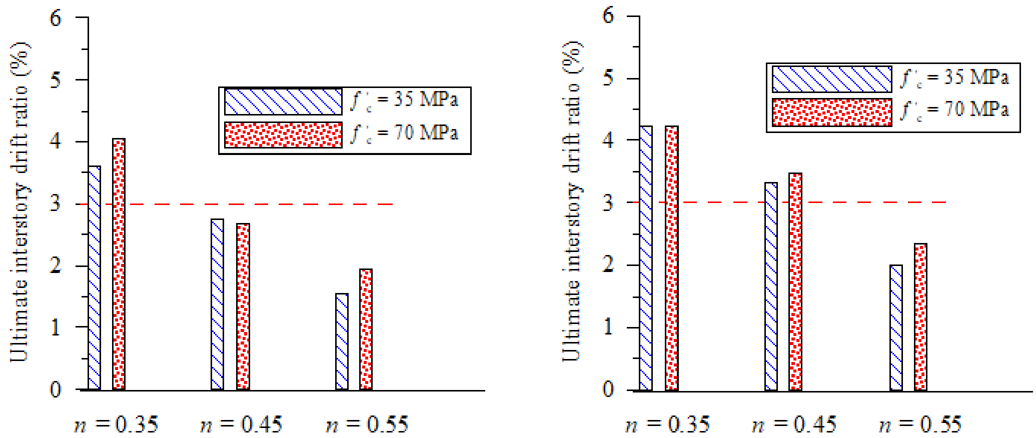

(a) Specimens with $B/t = 28$

(b) Specimens with $B/t = 21$

Figure 14. Effect of concrete strength on columns' deformation

4. Conclusions

Based on the numerical analyses of the seismic behavior of square CFST columns in this study, the main conclusions are drawn as bellow:

An FEA model was successfully developed in ABAQUS software for modeling square CFST columns under cyclic lateral loading with different axial load levels. In which, a reasonable stress-strain model for steel tubes, called elastic and linear hardening plastic model, was selected. Also, a new confined concrete model was proposed for infilled concrete behavior, whose mechanical properties relate to the confinement effect offered by the steel tube.

The validated FEA model was further extended to conduct parametric studies of square CFST columns with some parameters such as axial load level, width-to-thickness ratio of steel tube, and infilled concrete strength. Numerical simulation has demonstrated its effectiveness in time and cost expenditure compared to a corresponding experimental program. The numerical simulation results helped to disclose some significant findings as follows.

The higher the axial compression applied, the lower the shear strength and the IDR_u were. In particular, there was a dramatic shear strength reduction in the case of using thicker steel tube and lower strength concrete. Moreover, a dramatic IDR_u drop also was found when increasing axial load up to higher levels, especially, in the case of using thinner steel tube.

The B/t value strongly affects the column's strength and deformation capacity. It reveals that the smaller the B/t value, the higher the shear strength and the larger IDR_u were. The highest increase ratio in shear strength happened in the case of using lower strength concrete and the lowest axial load level. Moreover, the largest increase ratio in IDR_u happened in the case of using higher strength concrete and under the middle axial load level.

Increasing concrete strength leads to a dramatic increase in shear strength of the column in all cases. However, it results in both increase and light decrease in IDR_u depending on n and B/t value.

The study results also reveal that just the square CFST columns with thicker steel tubes (B/t = 21) have a good deformation capacity at two levels of axial load (n = 0.35 and 0.45) with their IDR_u larger than or equal to 3% radian (the building column's ductility demand in high seismic zones).

Acknowledgments

The author would like to send his thanks to The University of Danang – University of Science and Technology for the financial support to the Research project "Simulation of concrete filled steel tubular columns subjected to axial compressive and cyclic lateral loads", code number of Project: T2021-02-19.

References

[1] Phan, H. D., Lin, K.-C. (2020). Seismic behavior of full-scale square concrete filled steel tubular columns under high and varied axial compressions. *Earthquakes and Structures*, 18(6):677–689.
[2] Schneider, S. P. (1998). Axially loaded concrete-filled steel tubes. *Journal of structural Engineering*, 124 (10):1125–1138.
[3] Shams, M., Saadeghvaziri, M. A. (1999). Nonlinear response of concrete-filled steel tubular columns under axial loading. *Structural Journal*, 96(6):1009–1017.
[4] Susantha, K. A. S., Ge, H., Usami, T. (2001). Uniaxial stress–strain relationship of concrete confined by various shaped steel tubes. *Engineering Structures*, 23(10):1331–1347.
[5] Hu, H.-T., Huang, C.-S., Wu, M.-H., Wu, Y.-M. (2003). Nonlinear analysis of axially loaded concrete-filled tube columns with confinement effect. *Journal of Structural Engineering*, 129(10):1322–1329.
[6] Johansson, M., Gylltoft, K. (2002). Mechanical behavior of circular steel–concrete composite stub columns. *Journal of Structural Engineering*, 128(8):1073–1081.
[7] Liu, J., Zhou, X. (2010). Behavior and strength of tubed RC stub columns under axial compression. *Journal of Constructional Steel Research*, 66(1):28–36.
[8] Yu, Q., Tao, Z., Liu, W., Chen, Z.-B. (2010). Analysis and calculations of steel tube confined concrete (STCC) stub columns. *Journal of Constructional Steel Research*, 66(1):53–64.
[9] Phan, H. D., Trinh, H. H. (2017). Analysis of mechanical behaviour of circular concrete filled steel tube columns using high strength concrete. In *Proceedings of the 24th Australian Conference on the Mechanics of Structures and Materials (ACMSM24)*.
[10] Tao, Z., Wang, Z.-B., Yu, Q. (2013). Finite element modelling of concrete-filled steel stub columns under axial compression. *Journal of Constructional Steel Research*, 89:121–131.
[11] Thai, H.-T., Uy, B., Khan, M., Tao, Z., Mashiri, F. (2014). Numerical modelling of concrete-filled steel box columns incorporating high strength materials. *Journal of Constructional Steel Research*, 102:256–265.
[12] Han, L.-H., Tao, Z., Yao, G.-H. (2008). Behaviour of concrete-filled steel tubular members subjected to shear and constant axial compression. *Thin-Walled Structures*, 46(7-9):765–780.
[13] Liang, Q. Q. (2008). Nonlinear analysis of short concrete-filled steel tubular beam–columns under axial load and biaxial bending. *Journal of Constructional Steel Research*, 64(3):295–304.
[14] Abdullah, J. A., Sumei, Z., Jiepeng, L. (2010). Shear strength and behavior of tubed reinforced and steel reinforced concrete (TRC and TSRC) short columns. *Thin-Walled Structures*, 48(3):191–199.
[15] Moon, J., Lehman, D. E., Roeder, C. W., Lee, H.-E. (2013). Strength of circular concrete-filled tubes with and without internal reinforcement under combined loading. *Journal of Structural Engineering*, 139(12): 04013012.
[16] Hajjar, J. F., Gourley, B. C. (1996). Representation of concrete-filled steel tube cross-section strength. *Journal of Structural Engineering*, 122(11):1327–1336.

[17] Inai, E., Mukai, A., Kai, M., Tokinoya, H., Fukumoto, T., Mori, K. (2004). Behavior of concrete-filled steel tube beam columns. *Journal of Structural Engineering*, 130(2):189–202.
[18] Varma, A. H., Sause, R., Ricles, J. M., Li, Q. (2005). Development and validation of fiber model for high-strength square concrete-filled steel tube beam-columns. *ACI Structural Journal-American Concrete Institute*, 102(1):73–84.
[19] Zubydan, A. H., ElSabbagh, A. I. (2011). Monotonic and cyclic behavior of concrete-filled steel-tube beam-columns considering local buckling effect. *Thin-Walled Structures*, 49(4):465–481.
[20] Patel, V. I., Liang, Q. Q., Hadi, M. N. S. (2014). Numerical analysis of high-strength concrete-filled steel tubular slender beam-columns under cyclic loading. *Journal of Constructional Steel Research*, 92: 183–194.
[21] Skalomenos, K. A., Hatzigeorgiou, G. D., Beskos, D. E. (2014). Parameter identification of three hysteretic models for the simulation of the response of CFT columns to cyclic loading. *Engineering structures*, 61:44–60.
[22] Dat, P. X., Vu, N. A. (2020). An experimental study on the structural performance of reinforced concrete low-rise building columns subjected to axial loading. *Journal of Science and Technology in Civil Engineering (STCE)-NUCE*, 14(1):103–111.
[23] SIMULIA (2016). *Abaqus Analysis User's and Abaqus/CAE User's Guides*.
[24] Ellobody, E. (2013). Numerical modelling of fibre reinforced concrete-filled stainless steel tubular columns. *Thin-Walled Structures*, 63:1–12.
[25] AISC 360-16. *Specification for Structural Steel Building*. Chicago, Illinois, USA.